Dalton Transactions

ROYAL SOCIETY OF CHEMISTRY

PAPER

View Article Online
View Journal | View Issue

Cite this: *Dalton Trans.*, 2024, **53**, 7517

Unlocking single molecule magnetism: a supramolecular strategy for isolating neutral Mn^{III} salen-type dimer in crystalline environments†

Yuri Kyoya,[a] Kiyonori Takahashi, *[a,b] Wataru Kosaka, [c] Rui-Kang Huang, [a,b] Chen Xue, [a,b] Jia-bing Wu, [a,b] Hitoshi Miyasaka [c] and Takayoshi Nakamura*[a,b]

Received 2nd February 2024,
Accepted 2nd April 2024

DOI: 10.1039/d4dt00323c

rsc.li/dalton

In [Mn(5-MeOsalen)(Cl)]$_2$(dibenzo[24]crown-8), dibenzo[24]crown-8 formed a supramolecule *via* multi-point interactions with the [Mn(5-MeOsalen)(Cl)] dimer. The dimer was magnetically isolated with S_T = 4 and weak interdimer magnetic interactions. The crystal exhibited single-molecule magnet behaviour with an anisotropic barrier of 26(1) K, which is the highest among the Mn-salen series reported to date.

Introduction

Increasing the capacity of memory devices is essential for the development of information and communication technology. Magnetic recording media have also been miniaturized to increase their capacity. However, it has been pointed out that there is a limit to the miniaturization of conventional bulk magnets because they no longer behave as ferromagnetic materials when miniaturized to the nanoscale.[1,2]

Single-molecule magnets (SMMs), a group of materials in which single molecules on a nanoscale exhibit coercive force and behave as if they are magnets, are expected to be used in next-generation high-density recording devices and quantum computers. The magnetically isolated behaviour of molecules within a crystal is essential for displaying SMM behaviour. However, it can be challenging to control the magnetic isolation of cluster molecules, especially those that are electrostatically neutral clusters with a large spin ground state in a crystal packing.[3–5]

Our research group focused on a supramolecular strategy using crown ether derivatives for the isolation of molecules because the group of crown ether derivatives often acts as a "spacer" not only for spatial aspects in a crystal but also for through-space magnetic interactions. For example, the magnetically anisotropic polyoxometalate anion $\{[(PW_{11}O_{39})Dy(H_2O)_2]_2F\}$ is incorporated into the lattice structure formed by the (Na^+)benzo[18]crown-6 in the crystal to isolate each other. The magnetic exchange interaction between the anions was suppressed, and SMM behaviour was achieved.[6] If the supramolecular strategy based on crown ethers could be extended to electrostatically neutral SMMs, the versatility of the method would be enhanced for the isolation of a variety of SMMs and related compounds.

Crown ethers are capable of encapsulating electrostatically neutral molecules. The ether oxygen atoms in crown ether derivatives provide non-covalent electron pairs. In addition, highly electronegative oxygen atoms activate the neighboring carbon atoms. As a result, crown ethers can have diverse interactions with guest molecules at multiple points, such as C–H···O and C–H···π, in addition to the usual hydrogen bonding interactions, such as O–H···O and N–H···O. In the co-crystal of [18]crown-6 and adiponitrile, the C–H···O interactions between the CH_2 group of adiponitrile and the oxygen atom of [18]crown-6 asnd the C–H···π interactions between the π orbitals of the C≡N group of adiponitrile and the CH_2 group of [18]crown-6 stabilize the supramolecular structure.[7] Crown ethers with large rings are effective for the inclusion of large molecules. In the cocrystal of dibenzo[24]crown-8 (DB24C8) and neutral zinc tetrakis(4-hydroxyphenyl)porphyrin, the porphyrin molecule forms a supramolecule with DB24C8 and is isolated in the DB24C8 lattice. The zinc is coordinated by MeOH at the axial position, forming a square pyramidal geometry. DB24C8 covers the molecular face through hydrogen bonds between the MeOH and ether oxygen of DB24C8. The phenolic OH groups of the porphyrin molecule also interacted with DB24C8 molecules *via* hydrogen bonds, resulting in the zinc porphyrin being surrounded and isolated by DB24C8 in the crystal.[8]

In this study, we focused on an electrostatically neutral Mn-salen-type complex, [Mn(5-MeOsalen)(Cl)] (5-MeOsalen^{2-}:

[a]*Graduate School of Environmental Science, Hokkaido University, N10W5, Kita-Ward, Sapporo, 060-0810, Japan. E-mail: ktakahashi@es.hokudai.ac.jp, tnaka@es.hokudai.ac.jp*
[b]*Research Institute for Electronic Science (RIES), Hokkaido University, N20W10, Kita-Ward, Sapporo, 001-0020, Japan*
[c]*Institute for Materials Research (IMR), Tohoku University, 2-1-1 Katahira, Aoba-ku, Sendai 980-8577, Japan*

†Electronic supplementary information (ESI) available: Experimental section, details of single crystal X-ray analysis, powder X-ray diffraction, magnetic properties. CCDC 2329659. For ESI and crystallographic data in CIF or other electronic format see DOI: https://doi.org/10.1039/d4dt00323c

N,*N*′-ethylenebis(5-methoxysalicylideneiminate)), which is expected to form a self-assembled out-of-plane dimer to realize an SMM response if it could be magnetically isolated in the crystal. Mn-salen complexes are excellent SMM candidates because of their high ground-state spin with an $S_T = 4$ ground state and large uniaxial magnetic anisotropy involving tetragonal Jahn–Teller distortion with a large negative zero-field splitting parameter (D). However, SMM behaviour has recently been reported in co-crystals of a Zn_2Dy_2 Schiff base tetranuclear complex and binol derivatives, such examples are rare.[9] Considering the size of the molecule, DB24C8 was chosen as an aptamer to isolate the neutral dimer form of [Mn(5-MeOsalen)(Cl)] as [Mn(5-MeOsalen)(Cl)]$_2$(DB24C8) (**1**). A supramolecular assembly based on multipoint interactions was achieved between the [Mn(5-MeOsalen)(Cl)] dimer and DB24C8 in a crystal, in which the SMM behaviour of the dimer of [Mn(5-MeOsalen)(Cl)] was characteristically isolated.

Results and discussion

Crystal structure

The crystal system and space group of crystal **1** were triclinic and $P\bar{1}$, respectively. In the crystal, a [Mn(5-MeOsalen)(Cl)] molecule and half of the DB24C8 molecule were crystallographically independent. The N_2O_2 unit of the 5-MeOsalen ligand coordinates to the equatorial position of the Mn atom with interatomic Mn···O and N distances in the range from 1.883(3) to 2.006(4) Å, while Cl occupies the axial position within [Mn(5-MeOsalen)(Cl)] with Cl···Mn distance of 2.397(1) Å (interatomic distances and angles are summarized in Table S2 in ESI†). This apical-elongated square pyramidal configuration is typical for Mn^{III} high-spin complex characterized by Jahn–Teller distortion. The [Mn(5-MeOsalen)(Cl)] moiety was arranged in an out-of-plane dimer motif with intradimer O–Mn···O* angle of 86.6(1)°, and intradimer Mn···O* and Mn···Mn* distances of 3.914(3) and 4.2497(8) Å, respectively (*symmetry operation; 2 − x, 1 − y, 1 − z). According to the previous studies,[10–12] the observed O–Mn···O* angle was found in the typical case (77.83(5) − 91.069(16)°),[10] whereas the Mn···O* distance, as well as the Mn···Mn* distance, is much longer than typical Mn-salen type dimers (2.3698(16)–3.645(2) Å for Mn···O* and 3.3136(4) − 4.128(2) Å for Mn···Mn*).[10] Nevertheless, this distance is adopted in the range that derives ferromagnetic exchange interaction to yield $S_T = 4$ ground state.[10]

Fig. 1a shows the packing arrangement of crystal **1** as viewed along the [01−1] direction. [Mn(5-MeOsalen)(Cl)] dimers were arranged one-dimensionally in the open [01−1] direction. The [Mn(5-MeOsalen)(Cl)] dimer and DB24C8 are arranged alternately along the a-axis. The dimer was surrounded by two DB24C8 molecules from the [120] and [102] directions, in addition to those sandwiched along the a-axis (Fig. 1b). The six surrounding DB24C8 molecules effectively isolated the [Mn(5-MeOsalen)(Cl)] dimer. Fig. 2a shows the supramolecular interactions between the [Mn(5-MeOsalen)(Cl)] dimer and neighbouring DB24C8 along the a-axis.

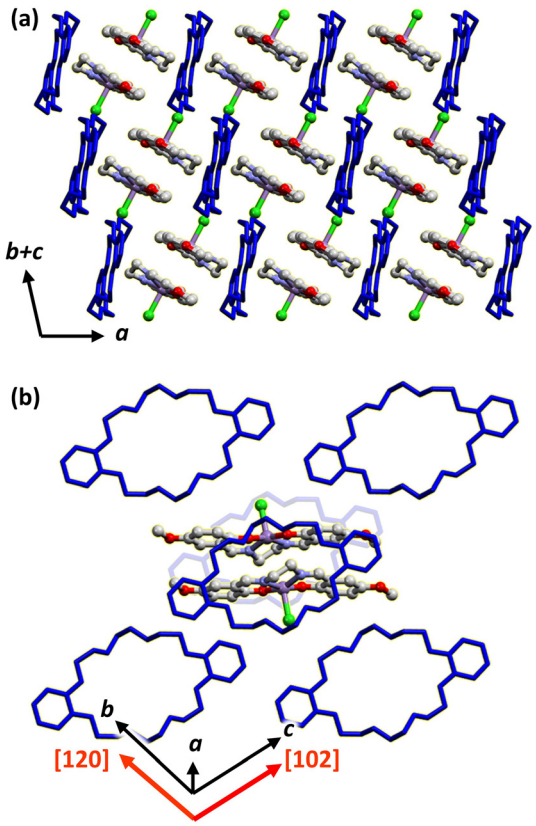

Fig. 1 Molecular arrangement in crystal **1**. [Mn(5-MeOsalen)(Cl)] and DB24C8 are represented by the ball-and-stick and stick models, respectively, where carbon, oxygen, nitrogen, chlorine, and manganese atoms in [Mn(5-MeOsalen)(Cl)] are denoted by gray, red, pale blue, yellowish green, and purple spheres, respectively, while DB24C8 is represented in blue. H atoms were omitted for clarity. (a) The [01−1] projection of the packing arrangement. (b) The [Mn(5-MeOsalen)(Cl)] dimer and six adjacent DB24C8 units viewed along the [100] direction.

Magnetic interactions within the [Mn(5-MeOsalen)(Cl)]dimer are restricted and the supramolecule is formed as a result of multipoint C–H···O interactions between the four hydrogen atoms attached to the ethylene chain in 5-MeOsalen and ether oxygens of DB24C8. The distances and angles of C–H···O bonds are summarized in Table S3.† Fig. 2b shows the interactions of [Mn(5-MeOsalen)(Cl)] with the neighbouring DB24C8 in the [120] and [102] directions. The ethylene chain of DB24C8 in the [120] direction has C–H···π and C–H···O interactions with the phenylene ring and terminal methoxy group, respectively, of [Mn(5-MeOsalen)(Cl)]. The ethylene chain of DB24C8 along the [102] direction also interacted with the terminal methoxy group. We quantitatively evaluated the stabilization energy between [Mn(5-MeOsalen)(Cl)] and the neighbouring DB24C8 molecule along the a-axis. DFT calculations with B3LYP-D2/6-31G(d,p) as the basis function reveal a stabilization energy of −128.4 kJ mol^{-1} for [Mn(5-MeOsalen)(Cl)]···DB24C8 pair. In general, the stabilization energies associated with C–H···O interactions are modest, and such interactions are considered unsuitable for promoting supramolecular formation. However, the value is more than one-

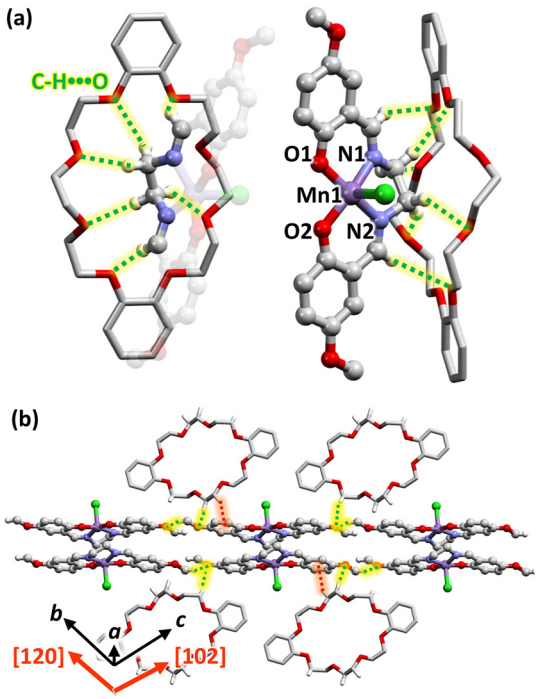

Fig. 2 Representation of intermolecular interactions between [Mn(5-MeOsalen)(Cl)] and DB24C8 and between [Mn(5-MeOsalen)(Cl)] dimers, where carbon, hydrogen, oxygen, nitrogen, chlorine, and manganese atoms are represented by gray, white, red, pale blue, yellowish green, and purple spheres, respectively. Hydrogen atoms that were not involved in the intermolecular interactions were excluded for clarity. C–H···O and C–H···π interactions are indicated by green and red dashed lines, respectively. (a) C–H···O interactions between [Mn(5-MeOsalen)(Cl)] and DB24C8 along the *a*-axis. (b) A one-dimensional array of [Mn(5-MeOsalen)(Cl)] dimers viewed along the [100] direction and DB24C8 surrounding the dimer.

third of the typical supramolecule of (K^+)18C6 (−300.3 kJ mol^{-1})[13] and (NH_4^+)18C6 (−314 kJ mol^{-1}),[14] and comparable to the supramolecule of 18C6 and a neutral molecule, benzenesulfonate amide (−104.2 kJ mol^{-1}).[15] [Mn(5-MeOsalen)(Cl)] and DB24C8 were assembled as a supramolecule in the crystal. On the other hand, the C–H···O and C–H···π interactions between DB24C8 and [Mn(5-MeOsalen)(Cl)] show relatively small stabilization energies of about −31.0 kJ mol^{-1} and −2.6 kJ mol^{-1} in the [120] and [102] directions, respectively.

Magnetic properties

Although the [Mn(5-MeOsalen)(Cl)] dimer is surrounded by six DB24C8 molecules, each dimer interacts with neighbouring dimers in the [01−1] direction *via* C–H···O between the terminal methoxy groups with C···O distance of 3.381(9) Å and C–H···O angle of 143.0°. Furthermore, the phenyl ring of the [Mn(5-MeOsalen)(Cl)] dimer was in contact with that of a neighbouring dimer in the *b* + *c* axis direction with the shortest C···C distances of 3.389(6) Å and centroid distance of 5.157 Å for the two phenylene rings (Fig. 2(b) and S3†). However, the spin density is localized at the Mn and N_2O_2 units, forming coordination spheres,[16] which DB24C8 covers from the *a*-axis direction and prevents intermolecular magnetic interactions. Since [Mn(5-MeOsalen)(Cl)] dimers contact each other only at the phenylene or methoxy groups, the magnetic interactions between dimers are weak, and the dimers should be magnetically isolated.

The temperature-dependent molar magnetic susceptibility (χ_m) of the polycrystalline sample of **1** (Fig. S4(a)†) indicates that the [Mn(5-MeOsalen)(Cl)] dimer had a high-spin ground state with an S_T = 4. The magnetization curve at 1.8 K (Fig. S4(b)†) was used to roughly estimate the magnetic parameters of intermolecular magnetic exchange interaction (zJ)

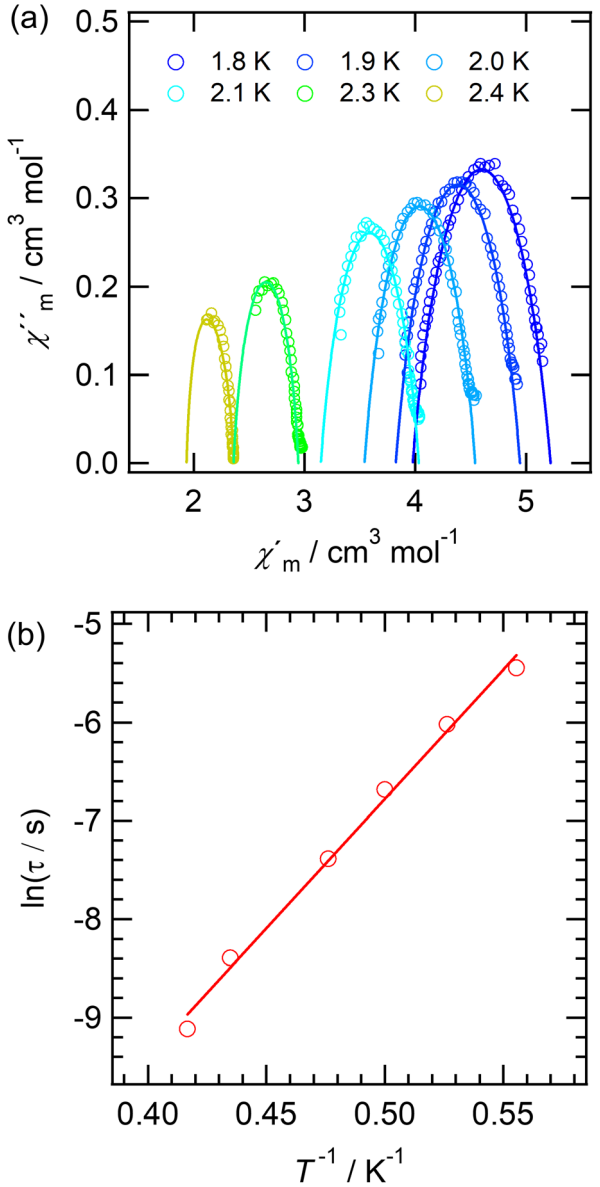

Fig. 3 (a) Cole–Cole plot between real (χ'_m) and imaginary (χ''_m) parts of AC susceptibility. The solid lines are least-squares fits employing the generalized Debye model. (b) Relaxation time (τ) *versus* 1/T deduced from the Cole–Cole plot. The solid red line represents the fit of the Arrhenius law.

and the zero-field splitting parameter (D). The zJ was estimated to be −0.20 K from

$$g\mu_B H_{ex} S_T = 2zJ{S_T}^2$$

where g, μ_B, and H_{ex} (=12.0 kOe) represent the Landé g factor with g = 2.0 (fix), the Bohr magneton, and the external magnetic field giving the maximum value of dM/dH in the plot of dM/dH *versus* H, respectively.[10] The magnetization at 7 T was 6.84$N\mu_B$, which did not reach saturation (M_{sat} = 8$N\mu_B$ with g = 2.0). Since the Mn-salen dimer has strong uniaxial magnetic anisotropy, D for **1** was estimated to be −1.84 K based on the following equation,

$$2|D|{S_T}^2 = g\mu_B S_T H_a$$

where H_a (=104 kOe) is the magnetic field when the linear region of the magnetization curve is extrapolated to M_{sat}.[10]

Twelve Mn-salen crystals reported previously exhibited SMM behaviour at a zero static field, in which the observed ranges of zJ and for D were from −0.18 to −0.25 K and from −1.65 to −1.85 K, respectively.[10] The effective isolation of [Mn(5-MeOsalen)(Cl)] dimer using a supramolecular structure provided a relatively small value of zJ compared to previously reported Mn-salen-based SMMs.

Compound **1** exhibited SMM properties in the absence of a static magnetic field. Cole–Cole plots obtained from AC susceptibility measurements at 1.8–2.4 K are summarized in Fig. 3a. The details of the fitting parameters for each temperature are listed in Table S4.† As shown in Fig. 3b, the relaxation time (τ) shows thermally activated behaviour with parameters $\ln(\tau_0)$ = 19.9(5) and anisotropy barrier (U_{eff}) = 26(1) K, indicating that the magnetic relaxation in crystal **1** follows the Orbach process. The U_{eff} value of crystal **1** corresponds to a relatively large D value of −1.84 K estimated from the magnetization curve. Notably, U_{eff} = 26(1) K is the largest among Mn-salen type complexes showing SMM behaviour under zero magnetic field reported so far.[10,12]

Conclusions

The supramolecular structure between DB24C8 and the neutral complex of [Mn(5-MeOsalen)(Cl)] was stabilized by multipoint C–H···O interactions in the a-axis direction. In addition, the bulky DB24C8 molecules interact in the [120] and [102] directions with the [Mn(5-MeOsalen)(Cl)] dimers, effectively suppressing the magnetic interaction between the dimers and realizing SMM behaviour. The supramolecular strategy, which can be applied to a wide variety of complexes with large zero-field splitting parameters, whether ionic or neutral, is a powerful tool for realizing novel SMMs.

Author contributions

Y. K. performed the synthesis and crystallization of compound **1** under the guidance of J. W., Y. K., R. H., and C. X. analysed and interpretated the crystallographic data. Y. K. performed the DFT calculation. W. K. acquired the magnetic data. Y. K., H. M., and K. T. analysed and interpreted the magnetic data. T. N., K. T., and Y. K. conceived and compiled the idea for the research and analysed and interpreted all data. The first manuscript was written by Y. K., K. T., and T. N. and edited by all authors.

Conflicts of interest

There are no conflicts to declare.

Acknowledgements

We thank Ms Ai Tokumitsu of Global Facility Center, Hokkaido University for elemental analysis, and Dr Shuhei Fukuoka and Dr Satoaki Matsunaga of the Faculty of Science, Hokkaido University, for χ_m measurements. This study was financially supported by JSPS KAKENHI (grant no. JP22H00311), JSPS Joint Research Projects under the Bilateral Programs (grant no. 120197402 and 120207401), feasibility study program by young researchers under the project of "Crossover Alliance to Create the Future with People, Intelligence and Materials", and Research Program of "Network Joint Research Center for Materials and Devices", from the Ministry of Education, Culture, Sports, Science and Technology of Japan (MEXT). This work was also supported in part by JST, ACT-X Grant Number JPMJAX23DB, Japan.

References

1 D. N. Woodruff, R. E. P. Winpenny and R. A. Layfield, *Chem. Rev.*, 2013, **113**, 5110–5148.
2 M. Adamek, O. Pastukh, M. Laskowska, A. Karczmarska and Ł. Laskowski, *Int. J. Mol. Sci.*, 2024, **25**, 52.
3 Q. Wu, Y. Li, Y. Wang, R. Clérac, Y. Lu and E. Wang, *Chem. Commun.*, 2009, 5743–5745.
4 A. Cornia, M. Mannini, P. Sainctavit and R. Sessoli, *Chem. Soc. Rev.*, 2011, **40**, 3076–3091.
5 D. Aulakh, L. Liu, J. R. Varghese, H. Xie, T. Islamoglu, K. Duell, C. W. Kung, C. E. Hsiung, Y. Zhang, R. J. Drout, O. K. Farha, K. R. Dunbar, Y. Han and M. Wriedt, *J. Am. Chem. Soc.*, 2019, **141**, 2997–3005.
6 D. F. Wu, K. Takahashi, M. Fujibayashi, N. Tsuchiya, G. Cosquer, R. K. Huang, C. Xue, S. Nishihara and T. Nakamura, *RSC Adv.*, 2022, **12**, 21280–21286.
7 A. Elbasyouny, H. J. Brügge, K. von Deuten, M. Dickel, A. Knöchel, K. U. Koch, J. Kopf, D. Melzer and G. Rudolph, *J. Am. Chem. Soc.*, 1983, **105**, 6588–6577.
8 Y. Diskin-Posner, G. K. Patra and I. Goldberg, *Acta Crystallogr.*, 2002, **C58**, m344–m346.
9 C. M. Liu, R. Sun, X. Hao and B. Wang, *Cryst. Growth Des.*, 2021, **21**, 4346–4353.

10 C. K. Terajima, R. Ishii, Y. Tojo, M. Fukuda, Y. Kitagawa, M. Asaoka and H. Miyasaka, *J. Phys. Chem. C*, 2017, **121**, 12454–12468.
11 H. Miyasaka and R. Clérac, *Bull. Chem. Soc. Jpn.*, 2005, **78**, 1725–1748.
12 H. Miyasaka, R. Clérac, W. Wernsdorfer, L. Lecren, C. Bonhomme, K. Sugiura and M. Yamashita, *Angew. Chem., Int. Ed.*, 2004, **43**, 2801–2805.
13 E. D. Glendening, D. Feller and M. A. Thompson, *J. Am. Chem. Soc.*, 1994, **116**, 10657–10669.
14 K. J. Hintze, A. Lützen and T. Bredow, *J. Comput. Chem.*, 2015, **36**, 1467–1472.
15 M. W. Shi, S. P. Thomas, G. A. Koutsantonis and M. A. Spackman, *Cryst. Growth Des.*, 2015, **15**, 5892–5900.
16 F. Teixeira, R. Mosquera, A. Melo, C. Freire and M. N. D. S. Cordeiro, *Int. J. Quantum Chem.*, 2014, **114**, 525–533.